THE AMERICAN SOCIETY OF MECHANICAL ENGINEERS
345 E. 47th St., New York, N.Y. 10017

96-GT-542

HEAT TRANSFER MEASUREMENTS TO A GAS TURBINE COOLING PASSAGE WITH INCLINED RIBS

Z. Wang and P.T.Ireland
Department of Engineering Science,
University of Oxford, Parks Road,
Oxford, OX1 3PJ

S.T.Kohler and J.W.Chew
Rolls Royce PLC, P.O.Box 3,
Filton, Bristol. BS12 7QE.

ABSTRACT

The local heat transfer coefficient distribution over all four walls of a large scale model of a gas turbine cooling passage have been measured in great detail. A new method of determining the heat transfer coefficient to the rib surface has been developed and the contribution of the rib, at 5% blockage, to the overall roughened heat transfer coefficient was found to be considerable. The vortex dominated flow field was interpreted from the detailed form of the measured local heat transfer contours. Computational Fluid Dynamics calculations support this model of the flow and yield friction factors which agree with measured values. Advances in the heat transfer measuring technique and data analysis procedure which confirm the accuracy of the transient method are described in full.

Nomenclature

a,b	constants in equations 8 and 9
c	specific heat capacity, J/kgK
d	passage dimension (0.05), m
f	friction factor
h	heat transfer coefficient, W/m^{2}K
l	coating thickness (equivalent to rib height), m
k	thermal conductivity, W/mK
p	pressure, N/m^2
q	heat flux, W/m^2
t	time, s
T	temperature, °C
U	response to delayed step or average velocity m/s
x	distance in flow direction, m

Greek

b_c	coating capacity
r	density, kg/m^3

Subscripts

aw	adiabatic wall
c	conducting rib
cl	centreline
o	initial
r	rough wall
s	perspex surface
w	wall

Presented at the International Gas Turbine and Aeroengine Congress & Exhibition
Birmingham, UK — June 10-13, 1996
This paper has been accepted for publication in the Transactions of the ASME
Discussion of it will be accepted at ASME Headquarters until September 30, 1996

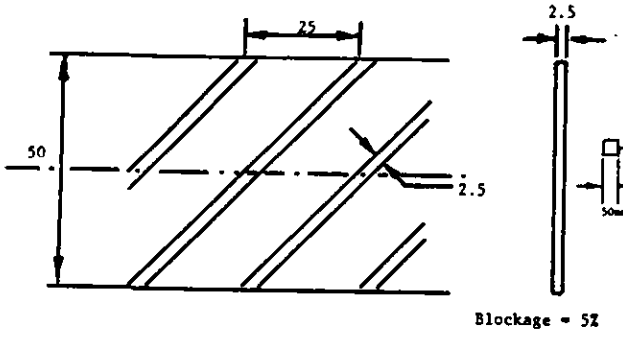

Figure 1 Rib roughness geometry applied to two facing walls of the passage. Ribs extend continuously from smooth wall to smooth wall.

Introduction

Countless different schemes have been adopted by engine manufacturers to cool the blades and vanes used in modern gas turbines: Sometimes, metallic inserts are used to partition the inside of hollow aerofoils to enable jets of coolant to be directed at the internal surface. Impingement cooling has received a great deal of research attention over the years and comprehensive reports by Florschuetz et al. (1981), Andrews et al. (1993) and, more recently, Van Treuren et al. (1996) number amongst those in the literature. Another frequently applied cooling strategy uses one or more cast passages which snake back and forth inside the blade. In some cases, the external heat load is so high that the cooling performance of the internal passage needs to be improved by casting roughness elements into the walls. The boundary layers on the passage walls are interrupted by roughness elements, such as ribs, and the heat and momentum processes enhanced by additional turbulence and secondary flows. Over the past decade or so, J. C. Han and his co-workers have produced a large data set to be used for the prediction of heat transfer and pressure drop in ribbed passages - see for example Lau et al. (1990). Holographic interferometry was used by Lockett and Collins (1990) to investigate the temperature field around square and rounded ribs set orthogonal to the flow direction. They reported normalised Nusselt number distributions over the complete surface of ribs at 6.7% blockage. Liou and Hwang (1993) used holography to study the effect of rib shape on heat transfer. Taslem and Wadsworth (1994) measured the contribution of rib heat transfer to the overall heat transfer using separately heated ribs in steady state experiments. They tested configurations in which the ribs were set at 90° to the flow direction and assessed the effect of rib pitch.

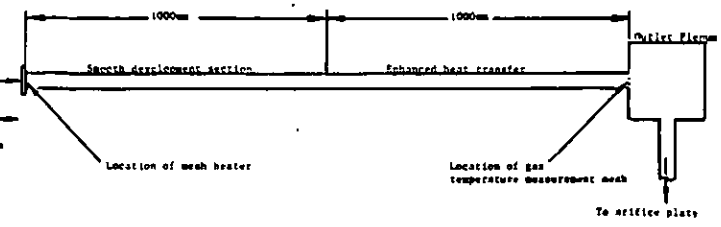

Figure 2 Experimental apparatus

The present research has investigated a simple form of roughness element used in aeroengines. Inclined ribs have been added to two facing walls of a square section passage The rib height is 5% of the passage hydraulic diameter and they are inclined at 45° to the passage major axis at a pitch of 10 rib sizes, Figure 1. The ribs, on the opposite walls, are inline and hence the minimum passage space gap is 80% of the passage hydraulic diameter. This geometry and blockage was chosen for two reasons. Firstly, it is typical of a configuration used in a particular aeroengine and the results were of direct interest to the designers. Secondly, data were available for the same geometry from the experiments of J. C. Han and his co-workers. The new means of determining the rib heat transfer coefficient, computing the flow field, using the heater mesh and employing the adiabatic wall temperature in the analysis could then assessed by comparison to the results of these authors. Once the experimental steps were verified, as reported below, the complete technique was applied in a rib roughness optimising programme for Rolls-Royce PLC. The present results are also significant in that the transient technique has been used to measure local heat transfer coefficients over the complete passage internal surface. This allows interpretation of the flow field in the light of complete surface data.

Experimental apparatus

The experimental apparatus is shown in Figure 2 and consists of a square cross-section (50mm × 50mm) duct 2000mm long. The first half of the duct is completely smooth walled and allows the hydrodynamic and thermal boundary layers to develop ahead of the second rib roughened half. This is representative of a ribbed passage in a turbine blade fed from a smooth section through the blade root. The large scale (approximately 20 ×) enables engine Reynolds numbers to be achieved at low speed and atmospheric pressure. The heat transfer results referred to in the following were taken in a position of

developed flow more than 15d from the start of the ribbed section. The issue of modelling small cast passages at large scale with smooth materials has been addressed by the authors (Wang et al., 1991). Coatings of sand and copper, with scaled average roughness values, R_a were used to measure the effect of engine representative roughness (R_a of order 1μm) on heat transfer levels. The results showed that the roughness caused by the casting process could significantly affect the heat transfer and pressure drop in small cooling passages. However, for the engine passages modelled in the present work, which were of order 5mm in hydraulic diameter, the casting roughness would have produced a second order influence relative to the large (≈250μm high) ribs.

Experimental technique

Conventional transient heat transfer method.

The transient heat transfer method has been applied by the authors to many different blade cooling problems. Its use was pioneered at Oxford by Jones, see Clifford et al. (1983), and recent developments are discussed in detail in Ireland et al. (1995). It offers the significant advantage of yielding local heat transfer coefficients over complete test surfaces in a single experiment. The technique relies on interpreting the thermal response of an insulating model to a change in fluid to model temperature difference. In the present research, a new means of producing the air temperature change was employed. A fine, fast response, mesh heater[1] was fitted to the duct inlet to produce the step change in gas temperature. This heater comprises a mesh of stainless steel wires, 40μm in diameter woven at a pitch of approximately 100μm. The tiny heat transfer passages constitute a highly effective heat exchanger with a convective efficiency[2] , over the range of speeds used in these tests, of more than 50%. This means that the mesh can run comparatively cool when supplying air heated by approximately 50°C. The heater time response is a function of the flow velocity and has been quantified by Gillespie et al. (1996). In the present experiments, the time constant was always less than 0.030s. In fact, the analysis of the crystal time response can be extended to account for a the heater time constant, Gillespie et al. (1996), though this was not required in the present experiments.

[1] UK patent application 9517643.4

[2] convective efficiency = actual heat transfer/ ideal heat transferred

The gas temperature was measured on the duct centreline at the axial location of the ribs. Conventional analysis that used the full gas temperature history was employed to determine the heat transfer coefficient at the site of a surface thermocouple applied to the perspex beneath the liquid crystal coating. It can be shown that, when the gas temperature change can be expressed as series of *n* summed step functions, the perspex surface temperature rise is

$$T - T_o = \sum_{i=1}^{i=n} (T_i - T_{i-1}) U(t - t_i) \qquad 1$$

where

$$U(t - t_i) = 1 - \exp\left(\frac{h_{cl}^2 (t - t_i)}{\rho c k}\right) erfc\left(\frac{h_{cl}\sqrt{t - t_i}}{\sqrt{\rho c k}}\right) \qquad 2$$

and T_i is the gas temperature at the *ith* step. An iterative procedure is used to determine the value of the heat transfer coefficient in the above equation (the only unknown) that gives the best agreement to the measured perspex surface temperature. The success of the fitting approach is demonstrated in Figure 3 where the values plotted as hollow circles are calculated using the best values of h_d (114W/m^{2}K) and T_d was approximated using a series of steps. Measured inlet and local centreline gas temperatures are also included in this figure together with a calculated surface temperature using adiabatic wall temperature and a different local heat transfer coefficient. The latter is discussed in the next section. The adiabatic wall temperature for the entire apparatus is the gas temperature at the inlet to the passage. The fast response heater ensures that this undergoes a step change at the start of the test and the familiar analytical solution

$$\frac{(T_s - T_0)}{(T_{aw} - T_0)} = 1 - \exp\left(\frac{h_{aw}^2 t}{\rho c k}\right) erfc\left(\frac{h_{aw}\sqrt{t}}{\sqrt{\rho c k}}\right) \qquad 3$$

for surface temperature, T_s, can be used in a regression procedure to determine *both* h_{aw} and adiabatic wall temperature from the measured surface temperature. The values of these two parameters which give the closest fit to the recorded wall temperature thermocouple signal are determined iteratively. The data points shown as the *s

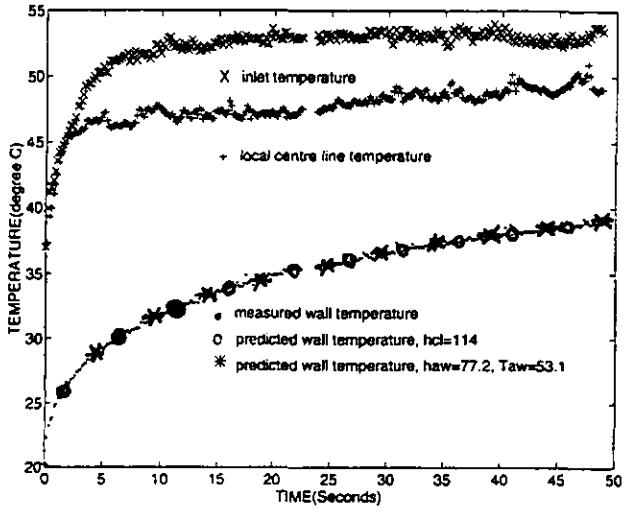

Figure 3 Surface temperature calculated from the best fit values of h_{cl} and T_{aw} using equation 1

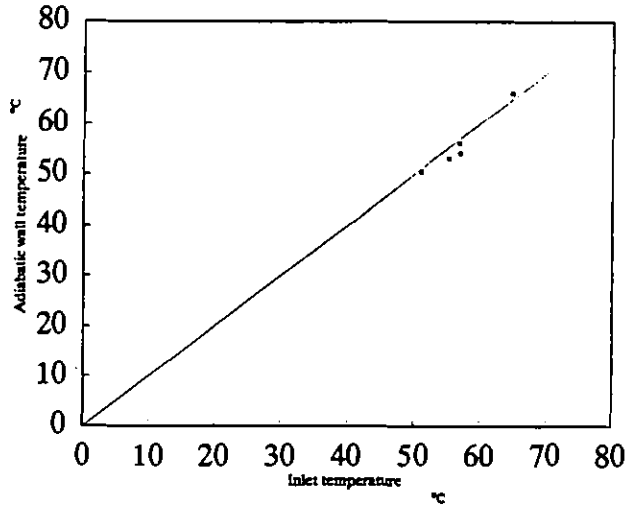

Figure 4 Adiabatic wall temperature determined from the surface temperature variation compared to the gas temperature immediately downstream of the mesh perspex model initial temperature. The centreline temperature is then calculated from Equation 4

in Figure 3 were calculated using this approach. In all of the experiments considered here, the adiabatic wall temperature was calculated and found to be within 2°C of the gas temperature measured on the gas temperature immediately downstream of the mesh heater. The agreement between these temperatures for typical tests is demonstrated in Figure 4.

The use of adiabatic wall temperature to confirm data integrity.

The local heat transfer coefficient based on the adiabatic wall temperature was also calculated and used as a check on the accuracy of the data. This heat transfer coefficient is significantly different to that based on the local centreline temperature (e.g. 77.2 and 114 respectively in Figure 3). As explained above, the latter was determined from the continuous record of the gas temperature using a regression procedure in which only h_{cl} was varied to produce the best fit for surface temperature calculated from the summed step change solution. Since the local heat flux at the thermocouple can be expressed in terms of either gas temperature,

$$q = h_{cl}\left(T_{cl} - T_w\right) = h_{aw}\left(T_{aw} - T_w\right) \qquad 4$$

at a time when the wall temperature is known, the centreline temperature can be determined from the adiabatic wall temperature and heat transfer coefficient ratio. At the start of the test, the wall temperature is the perspex model initial temperature. The centreline temperature is then calculated from

$$T_{cl} = T_w\left(1 - \frac{h_{aw}}{h_{cl}}\right) + \frac{h_{aw}}{h_{cl}} T_{aw} \qquad 5$$

The starting temperature measured at the gas thermocouple was then compared to that calculated from the above equation. Figure 5 is a plot of the starting gas temperature determined both ways. The agreement is further evidence that the experimental measurements of h_{cl} are accurate.

Image processing

Conventional 'hue scaling' as invented by Wang (Wang et al., 1994, 1995) was used to determine the local heat transfer values over the perspex surface between the ribs. In this method, the heat transfer coefficient divided by a reference heat transfer coefficient is calculated at each pixel. The uncertainty in measured heat transfer coefficient ratio is very small (less than 1%). The reference heat transfer coefficient is calculated from the full thermal transient measured using a surface thermocouple.

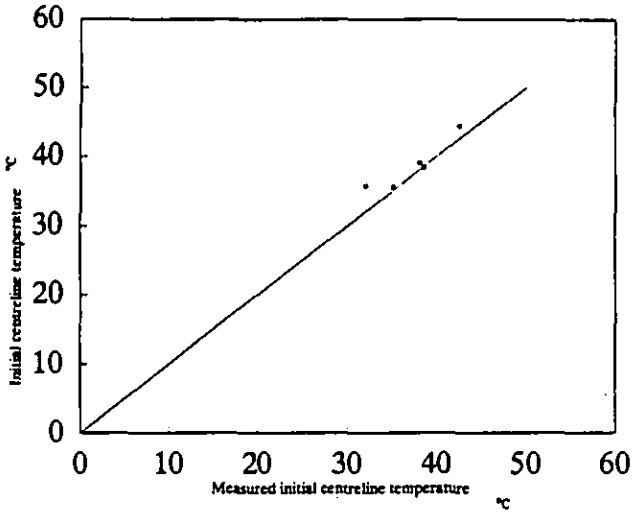

Figure 5 Starting centreline gas temperature (at the instrumented rib location) determined from equation 5 compared to the measured value

Rib roughness heat transfer measurement

A new approach to determining the rib heat transfer coefficients has been invented. Metallic ribs were glued to the encapsulated liquid crystal coated perspex inner surface and analysis which accounts for the rib heat capacity used to determine the effective heat transfer coefficient acting at the rib base. The high conductivity of the copper rib acts to keep the rib temperature uniform as the transient test proceeds. An assessment of the influence of variation in heat transfer coefficient along the rib length on the average *h* measured was made to confirm the accuracy of the approach. A numerical solution to the transient conduction equation in two dimensions was used to demonstrate that the average h, for realistic distributions of h, was the achieved in the presence of conduction along the rib.

The effective heat transfer coefficient for the ribs was determined using the analysis developed at Oxford for grain roughness heat transfer measurements, Wang et al. (1991). The roughness surface temperature rise for a step change in gas temperature is related to the effective heat transfer coefficient, h, and the coating capacity , β_c defined as

$$\beta_c = \rho_c c_c l\left(1 - \frac{hl}{2k_c}\right) \qquad 6$$

by

$$\frac{T(0,t) - T_o}{T_g - T_o} = 1 + h\left(\frac{\exp(a^2 t)erfc(a\sqrt{t})}{\beta a(a-b)} - \frac{\exp(b^2 t)erfc(a\sqrt{t})}{\beta b(b-a)}\right)^7$$

where

$$a = \frac{\sqrt{\rho ck}}{2\beta_c}\left(1 + \sqrt{1 - \frac{4\beta_c h}{\rho ck}}\right) \qquad 8$$

and

$$b = \frac{\sqrt{\rho ck}}{2\beta_c}\left(1 - \sqrt{1 - \frac{4\beta_c h}{\rho ck}}\right) \qquad 9$$

The contribution to the overall heat transfer of heat convected at the rib surface has been known to be important for some time and is referred to in Shen et al. (1994). It should be noted that the ribs, as well as turbulating the flow, act as devices for extending the internal surface of the duct.

Outlet gas temperature visualisation

A nylon mesh, coated with temperature sensitive liquid crystal, was fitted to the outlet of the duct to inspect the temperature field. The crystal colour display on the mesh is shown at two times , during a transient heat transfer test, in Figure 6. The use of these meshes is proving to be a very useful quantitative tool for investigating the temperature fields inside cooling passages- see Wang et al. (1996). The mesh used has a low porosity and produces a pressure drop of 8% of a dynamic head. For these experiments, it has been coated with encapsulated liquid crystals that show colour in the range 25°C to 33°C.

The temperature profile exhibits a narrow cooler zone (the gas is warmer than the perspex) which reaches from the smooth wall adjacent to the trailing edges of the

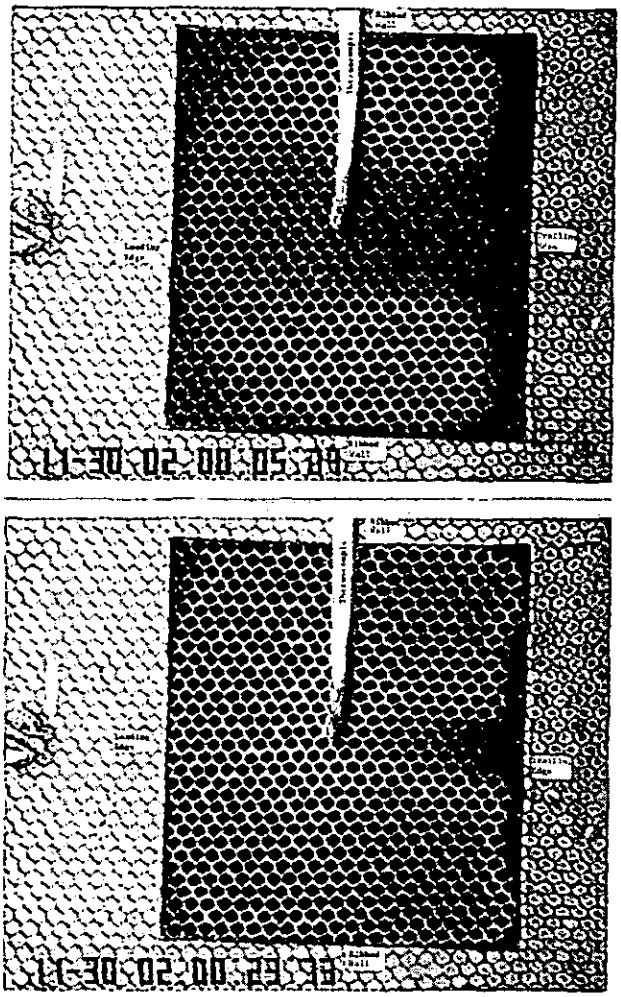

Figure 6 The liquid crystal colour play on the mesh fitted to the duct outlet at two instants during a transient experiment. (sampled over the mesh fibres) averaged across

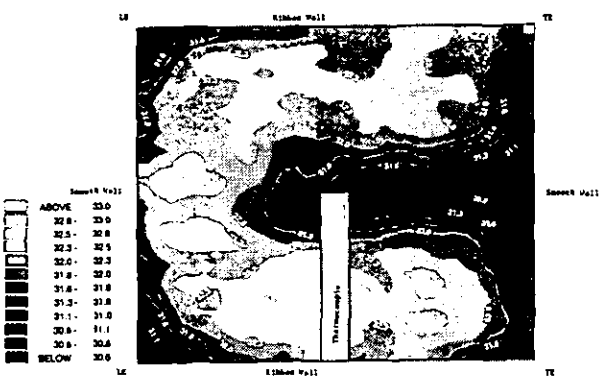

Figure 7 Gas temperature distribution over the mesh al 46.6 seconds after switching power to the heater.

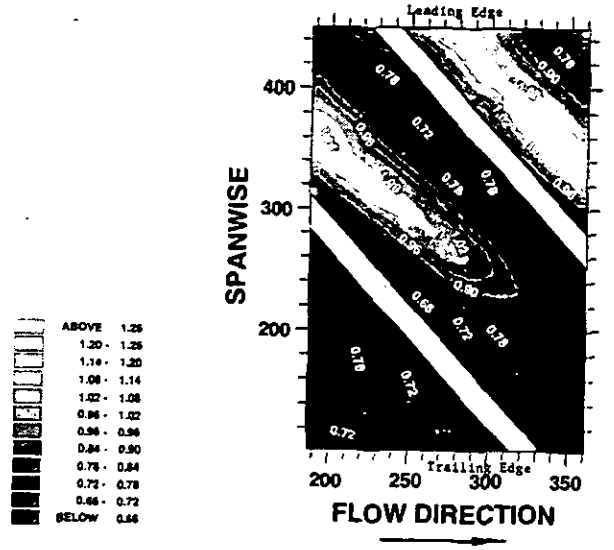

Figure 8 Heat transfer coefficient distribution on the surface between the ribs.

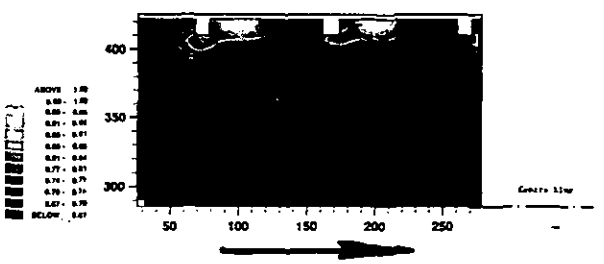

Figure 9 Heat transfer coefficient distribution on the smooth wall adjacent to leading edge of the ribs. The arrow indicates flow direction.

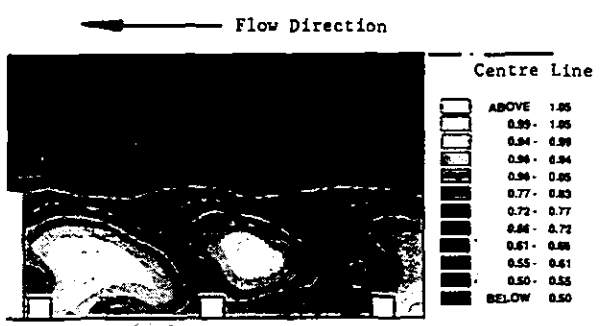

Figure 10 Heat transfer coefficient distribution on the smooth wall adjacent to trailing edge of the ribs. The arrow indicates flow direction.

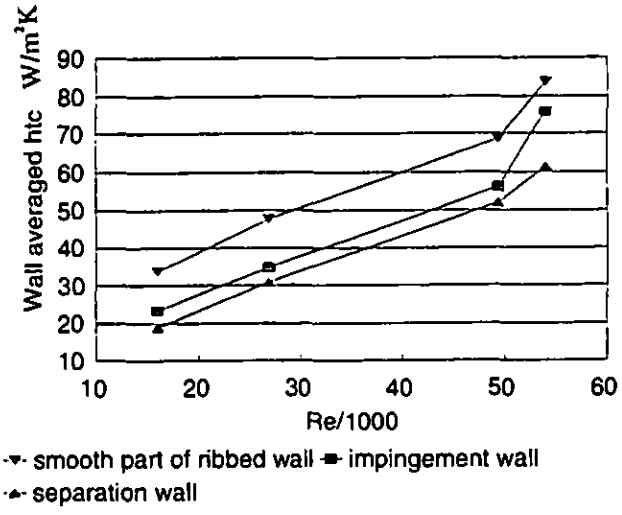

Figure 11 Comparison of smooth surface heat transfer coefficients.

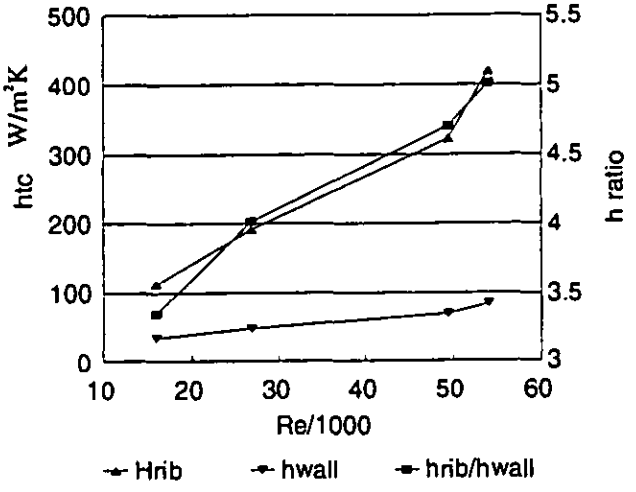

Figure 12 Rib heat transfer coefficient compared to the value on the smooth wall between the ribs.

inclined ribs, Figure 7. In fact, the mesh shows that the centreline temperature is *less* than the temperature of the passage. The use of crystal coated meshes to establish dimensionless temperature difference profiles is discussed in detail in Wang et al. (1996). The duct pressure loss measurements discussed below were performed without the crystal coated mesh fitted.

Heat transfer measurements

The local heat transfer coefficient on the surface

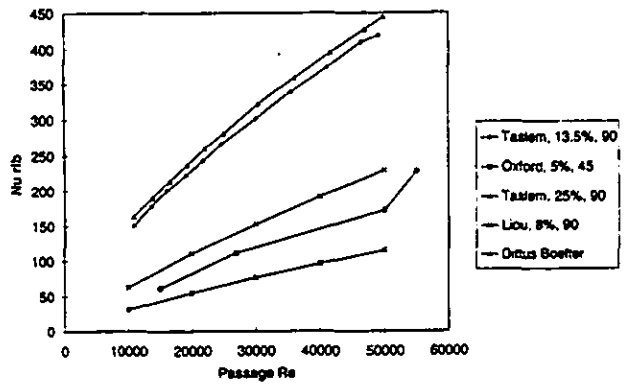

Figure 13 Average Nusselt number over the rib surface compared to data from the literature.

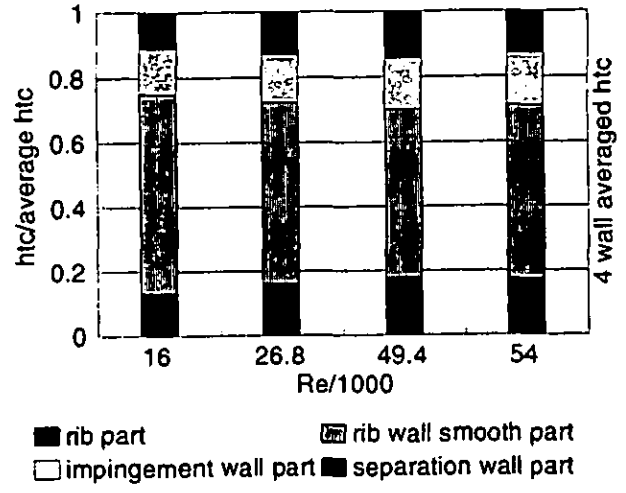

Figure 14 Contributions of the different surfaces to the complete passage heat transfer.

between the ribs is shown in Figure 8. A predominant feature is the high heat transfer region between the ribs Similar to 90° ribs, this high region is caused by the vortex structure between the ribs. It is interesting to note that in the direction parallel to the ribbes the distribution is far from uniform with a peak occurring towards the 'leading edge' of the parallel ribs. Heat transfer levels are presented in this figure normalised with respect to the value at the thermocouple. The local heat transfer values on the smooth walls are shown in Figure 9 and Figure 10 where the considerable enhancement close to the rib tops can be seen. Other features in Figures 8-10 are discussed later in conjunction with the result from a C.F.D. computation. The averaged values of the smooth wall *h*

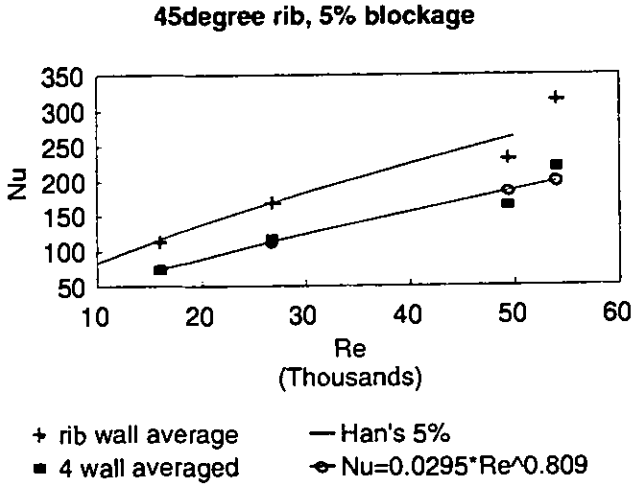

Figure 15 Ribbed passage rough wall Nusselt number as a function of Reynolds number.

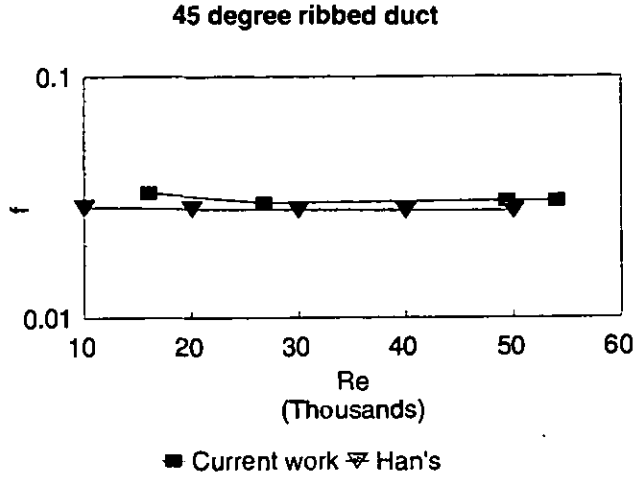

Figure 16 Measured friction factor as a function of passage Reynolds number

are shown in Figure 11 as a function of Reynolds number where comparison is also made to the level between the ribs. The rib h values are, as expected, much higher than the smooth levels and these are shown in Figure 12. This figure includes the ratio of rib to smooth surface value on the ribbed wall. The average rib Nusselt number as a function of duct Reynolds number is presented in Figure 13 where the length dimension is the passage diameter. The data from Taslem and Wadsworth, at relatively high blockage, was performed in apparatus in which only the rib was heated. The thermal boundary conditions are thus different from the essentially isothermal wall state prevailing during the present transient tests. This difference would be expected to increase the former data compared to the transient results.

Insight can be gained into the relative contributions of the different surfaces to the overall heat transfer from Figure 14. The appropriate surface areas have been used to determine this bar graph. The dimensionless, overall, rough-wall Nusselt number, is plotted as a function of Reynolds number in Figure 15 where comparison is made to the data from Texas A&M University. The data from Han et al. (1991) have been adjusted to yield values at the present blockage of 5% using the law of the wall roughness function (R and G) approach. Agreement to the present results is excellent, although it should be noted that the Texas heat transfer coefficients are based on the mixed bulk gas temperature and the present results are based on the local centreline temperature. Perhaps, the similarity between the results is not surprising when account is taken of the uniformity of temperature distribution shown in Figure 7. Analysis discussed in Wang et al. (1996) suggests that the Han data should be increased by approximately 8% to obtain Nusselt number values based on local centreline temperature.

Friction factor data

The static pressure was measured at different stations along the smooth passage wall for different Reynolds numbers. The friction factor defined as

$$f = \frac{1}{\frac{1}{2}\rho U^2} \frac{d}{4} \frac{dp}{dx} \qquad 10$$

was calculated from the measurements and is plotted in Figure 16. The results compare well with the line derived from the wall roughness functions after Han et al. (1991).

C.F.D. prediction

The flow field inside the passage was calculated using the simple drag coefficient model described in Chew et al. (1996). Here, the drag force due to the ribs, is included in the momentum equations as a source (or body force) term averaged over the length of the ribbed section of the duct. This is assumed to act normal to the rib and is evaluated from the product of the rib area, the dynamic head of the local flow velocity and an empirically determined coefficient. Secondary flows

established by the angle forces are apparent from the vectors presented in Figure 17. The values of friction factor derived were in good agreement with the measured data and will be reported later. The approach has been used successfully by Chew et al. (1996) to predict the variation of friction factor with rib inclination. C.F.D. predictions of the flow temperature field are also given in Figure 18

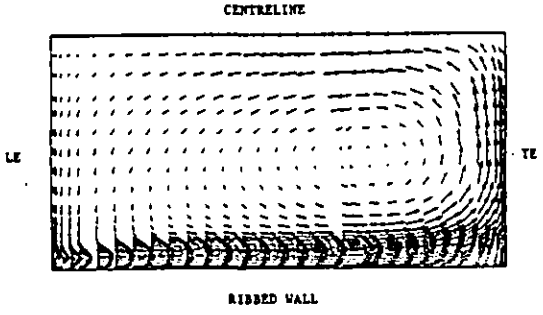

Figure 17 Secondary flows calculaled using the rib drag coefficient model reported in Chew et al. (1996).

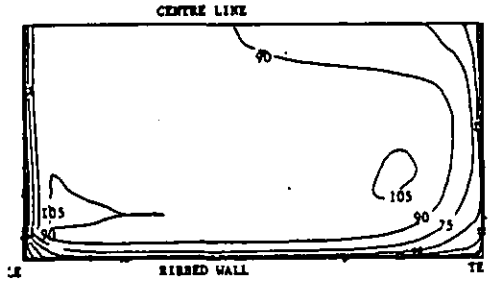

Figure 18 Thermal field calculated using the rib drag coefficient model reported in Chew et al. (1996). T_{avg}-T_w=100

Discusslon of results

The inclined ribs are expected to produce a pair of large counter rotating vortices as shown in the CFD results in Figure 17. These vortices convey fluid from the centre of the passage to the smooth wall adjacent to the leading edge of the ribs. The low cooling potential (temperature in the heat transfer experiment) at the core of the vortices is apparent from Figure 17. It seems that the classical flow field behind parallel ribs is significantly influenced by the secondary flows as the heat transfer coefficient contours here do not run parallel to the ribs, Figure 8. The reduction of the heat transfer level in the region close to the trailing edge is evident. This reduction may be explained, firstly, by the growth of the boundary layer in the secondary flow direction. The second possible reason for this reduction is the divergence and the `lift off' of the small vortex structure local to each rib. This phenomenon can be noted by comparing the size difference of the footprints of elevated heat transfer where the rib vortices interact with the smooth walls (Figure 9 and Figure 10). This trend can be explained by the counter rotating main vortices. On the leading edge smooth wall (Figure 9), the secondary flow is predominantly in the direction from the centreline towards the ribbed wall. This tends to compress the rib vortex towards the ribbed wall. Also note the local high heat transfer level at the centreline which is the consequence of the `impingement' of the twin large vortices. On the trailing edge smooth wall ( Figure 10 ) the secondary flow is from the ribbed wall towards the centreline. This has the effect of `lifting' and expanding the main rib vortex structure. The secondary flow is expected to change the flow conditions at which different flow phenomena occur. In particular, the condition for the onset of the classical `sealed' circulation between ribs at close spacing . Therefore the optimised rib pitch to height ratio for the inclined ribs is expected to differ from the established value of 10:1 for plain 90° ribs. This is clearly an important topic for future investigation.

Conclusions

1. The first local heat transfer coefficients over the complete surface of a typical inclined rib gas turbine cooling passage have been measured. The contours support a model of the flow field with two counter rotating major vortices.
2. Local values of h have been measured on the smooth surfaces. The highest heat transfer on these faces is observed close to the rib tops.
3. A new CFD prediction method has been used to calculate the flow field. The calculated secondary flows are consistent with the experimental data.
4. The transient heat transfer measuring technique has been advanced by introducing a hybrid model technique which uses copper conducting, isothermal, roughness elements in a perspex duct.
5. Sophisticated data analysis has been used to demonstrate the quality of the heat transfer data.

Acknowledgements

This work has been carried out with the support of the UK Ministry of Defence and DTI together with Rolls-Royce PLC. The technical assistance of Mr. P. J. Timms was also much appreciated. The liquid crystals were supplied by Hallcrest L.C.T.[3]

References

Andrews, G. E., Asere, A. A., Hussain, C. I., Mkpadi, M.C. and Nazadi, A.,1992," Impingement / effusion cooling," AGARD CP-527,. paper no. 30.

Chew, J. W., Taylor, I. J. and Bonsell, J. J., 1996, " CFD Developments for Turbine Blade Heat Transfer," 3rd International Conf. on Computers in Reciprocating Engines, I. Mech. E., London, 9-10 Jan. Paper C499-035.

Clifford, R. J., Jones, T.V. and Dunne, S. T., 1983, "Techniques for obtaining detailed heat transfer coefficient measurements within gas turbine blades and vane cooling passages," ASME paper 83-GT-58.

Florschuetz, L. W., Metzger, D. E. and Truman, C. R., 1981," Jet array impingement with crossflow- correlation of streamwise resolved flow and heat transfer distributions," NASA CR 3373.

Gillespie, D. R. H., Wang, Z., Ireland P. T. and Kohler, S. T., 1996," Full surface local heat transfer coefficient measurements in an integrally cast impingement cooling geometry," submitted for ASME Gas turbine conference, Birmingham.

Han, J. C., Zhang, Y. M. and Lee, C. P., 1991, " Augmented heat transfer in square channels with parallel, crossed and v-shaped angled ribs," Journal of Heat transfer, vol. 113, pp. 590-596.

Ireland, P. T., Wang, Z. and Jones, T. V., 1995," Liquid crystal heat transfer measurements," VKI lecture series *Measurement Techniques*, 1995-01.

Lau, S. C., McMillin, R. D. and Han, J.C., 1990," Heat transfer characteristics of turbulent flow in a square channel,"ASME paper 90-GT-254.

Liou, T. M. and Hwang, J.J., 1993, " Effects of ridge shapes on turbulent heat transfer and friction in a rectangular channel," International Journal of Heat and Mass Transfer, vol. 36, pp. 931-940.

Lockett, J. F. and Collins, M. W., 1990," Holographic interferometry applied to rib-roughness heat transfer in turbulent flow," Int. Journal of Heat and Mass Transfer, vol. 33 no. 11, pp. 2439-2449.

Taslem, M. E. and Wadsworth, C. M., 1994,"An experimental investigation of the rib surface-averaged heat transfer coefficient in a rib-roughened square passage," ASME paper 94-GT-162.

Shen, J-R, Ireland, P.T., Wang, Z. and Jones," Heat transfer enhancement within a turbine blade cooling passage using ribs and combinations of ribs with film cooling holes." *ASME paper 94-GT-232*, accepted for publication in the Journal of Turbomachinery.

Van Treuren, K. V., Wang, Z., Ireland P. T., Jones, T. V. and Kohler, S. T., 1996, " Comparison of local and average heat transfer coefficients under an array of inline and staggered impinging jets," submitted for ASME Gas turbine conference, Birmingham.

Wang, Z., Ireland, P. T. and Kohler, S. T., 1996," Gas temperature measurement in internal cooling passages," submitted for ASME Gas turbine conference, Birmingham.

Wang, Z., Ireland, P. T., Jones, T. V., and Davenport, R., 1994," A Colour Image Processing System For Transient Liquid Crystal Heat Transfer Experiments," *ASME Paper No. 94-GT-290*, accepted for publication in the Journal of Turbomachinery.

Wang, Z., Ireland, P.T. and Jones, T.V., 1995," An Advanced Method of Processing Liquid Crystal Video Signal From Transient Heat Transfer Experiments," *Trans. ASME-Journal of Turbomachinery,* Vol.117,, pp.184-189. Also ASME paper 93-GT-282.

Wang, Z., Ireland, P.T. and Jones, T.V., 1991," A Technique for Measuring Convective Heat Transfer at Rough Surfaces," *Trans.Inst Measurement and Control,* Vol.13, no. 3, pp.145-154.

[3] Hallcrest L.C.T., Unit 9, Stepnell Reach, 541 Blandworthy Road, Hamworthy, Poole, Dorset. BH16 5BW.